2020 IEEE/RSJ International Conference on Intelligent Robots and Systems (IROS)
October 25-29, 2020, Las Vegas, NV, USA (Virtual)

An Earthworm-like Soft Robot with Integration of Single Pneumatic Actuator and Cellular Structures for Peristaltic Motion

Mingcan Liu, Zhaoyi Xu, Jing Jie Ong, Jian Zhu, Wen Feng Lu*

Abstract— **Earthworm-like soft robots have been widely studied for various applications, such as medical endoscopy and pipeline inspection. Many actuation modes have been chosen to drive the soft robots, including pneumatic actuators, dielectric elastomeric actuators, and shape memory actuators. Pneumatic actuators stand out since the soft robots with pneumatic actuation can produce relatively large forces and displacements with relatively ease of fabrication. Currently, several pneumatic actuators are used to realize elongating movement and anchoring movement of the earthworm for peristaltic motion. More pneumatic actuators not only require more pumps and valves to actuate and control the earthworm, but also lead to less efficient movement control of the earthworm. To address this issue, a new design with integrated single pneumatic actuator and cellular structures is developed to realize elongating movement and anchoring movement of the earthworm-like soft robot in peristaltic motion. With the new design, the simulation model of the new earthworm is developed to simulate both elongating and anchoring movements of the earthworm. A 3D printed prototype of the earthworm-like soft robot is fabricated to validate the proposed design and simulation model. Experimental results show good agreement with the simulation in elongations of peristaltic motion as the differences between the simulated and experimental is 5.8 % in one cycle of the peristaltic motion.**

I. Introduction

Soft robots rely on the deformation of the body structure to interact with real-world environments [1]. By mimicking the structures of soft-bodied invertebrates, like jellyfish [2], octopus [3], caterpillar [4, 5], and earthworms [6], soft robots can be designed and used for a variety of domestic, industrial and medical applications. Inspired by earthworms' peristaltic crawling motion, earthworm-like soft robots have been widely developed for applications ranging from medical endoscopy [7] to pipeline inspection [8]. A real earthworm contracts and expands the longitudinal and circular muscle to achieve peristaltic motion [9]. To drive the earthworm-like soft robots, many actuations modes have been used, like pneumatic actuators [4], shape memory alloy actuators (SMAs) [10], and dielectric elastomeric actuators (DEAs) [11]. Compared with SMAs and DEAs, pneumatic actuators can achieve relatively larger forces and displacements inflated by air pumps and be easily fabricated by 3D printing.

*Corresponding author. Research supported by China Scholarship Council.

M. Liu, J. J. Ong, J. Zhu and W. F. Lu are with the Department of Mechanical Engineering, National University of Singapore, 9 Engineering Drive 1, Singapore 117575 (M. Liu – liumingcan@u.nus.edu; J. J. Ong – ongjingjie@u.nus.edu; J. Zhu – mpezhuj@nus.edu.sg; W. F. Lu – Tel: +65 6516 1228; email: mpelwf@nus.edu.sg).

Z. Xu is with the Department of Mechanical and Industrial Engineering, University of Toronto, Toronto, ON M5S 3G8, Canada (Z. Xu – zhaoyi.xu@mail.utoronto.ca).

The earthworm-like pneumatic soft robots often contains several pneumatic actuators to realize the elongating movement of central body and anchoring movement of setae. Zou et al. [4] used several modules to achieve crawling motion to crawl in a pipe. However, huge numbers of pneumatic actuators made control strategy of the system complicated. Qi et al. [12] designed four earthworm-like segments to achieve peristaltic motion, but the control of the peristaltic motion was less efficient. Even the simplest earthworm often needs three actuators; one for elongating motion, and two for front and rear anchoring motion, as proposed in [13]. More pneumatic actuators mean more pumps and valves are needed to actuate and control the earthworm. It will make the system more complicated and less effective to control the movement of the earthworm. Under this circumstance, earthworms with less pneumatic actuators are needed for a variety of applications. To reduce the actuators, one could look into the possibility of replacing the two pneumatic actuators for anchoring movement with alternative design. On the other aspect, cellular structures have been used in functional applications, such as fluid flow control and acoustic control as described in [14]. It should be interesting to explore the use of cellular structures for anchoring movement. Cellular structures are made of solid struts or plates on the edges and faces of the unit cells, including auxetic structures [15]. Auxetic structures [16] are a kind of special lattice structures with Negative Poisson's Ratio (NPR). If NPR structure is stretched (or compressed) in one direction, it will expand (or contract) in perpendicular directions. Cellular structures have been used in soft robotics to achieve different functions. Mark et al. [17] used auxetic metamaterials to simplify the design of two extremes to allow the soft robot to easily crawl in a vertical pipe. Hasse and Mauser [18] used nonuniform cellular structures to design a bending actuator for soft robots to realize turning motion. By designing the structure of cylindrical soft actuator, Lazarus and Reis [19] achieved flexural and twisting motion through auxetic behavior.

Based on the limitations, the objective of this paper is to develop a new design with integrated single pneumatic actuator and cellular structures for earthworms to achieve elongating and anchoring movements in peristaltic motion. With the new design, the simulation model of the new earthworm is developed to simulate both elongating and anchoring movement of the earthworm. A 3D printed prototype of the earthworm-like soft robot is fabricated to validate the proposed design and simulation. This paper attempts to simplify the actuation of the earthworm-like soft robot motion by integrating actuation with cellular structures.

II. Design and Fabrication

The proposed earthworm is similar to the soft robot in [20]; However, the proposed design uses cellular structures to

978-1-7281-6211-9/20/$31.00 ©2020 IEEE

integrate with actuation to reduce the use of the pneumatic actuator. In [20], the soft robot contained three parts, front extremal actuator, central body actuator and rear extremal actuator. The front and rear extremes were used for anchoring movement, while the central actuator was used for elongating movement. To achieve peristaltic motion, the friction modulation of two extremes with inflating and deflating the extremal actuators to shift the material contact with the ground surface is required.

A. Conceptual Design

In the proposed design, the earthworm also consists of three parts, the front extreme, the central body and the rear extreme. To reduce the use of actuators, the structures of two extremes have been redesigned to achieve anchoring movement under friction modulation. To achieve peristaltic motion, the central pneumatic actuator body extends and contracts to generate elongating movement. The pressure in the central body drives the two extremes to modulate the frictions needed to alternately anchor the robot to the ground. Fig. 1 shows the schematic diagram of the proposed earthworm with one pneumatic actuator and two extremes with cellular structures.

As shown in Fig.1, front extreme consists of a hard casing with Cellular Structure 1 (CS1) encased in it, while rear extreme consists of a hard casing with Cellular Structure 2 (CS2) encased in it. In order to modulate the friction of extremes with the ground, the material of two cellular structures should have high coefficient of friction with ground surface, while the material of two casings outside the cellular structures should have low coefficient of friction with ground surface. Cellular structures and casings both can produce frictions with the ground.

Before the movement, both CS1 and casing in the front extreme are in contact with the ground to produce high friction to anchor the front extreme. Casing in the rear extreme contacts the ground to produce low friction. To crawl forward, the central actuator is inflated, the actuation force f_a gradually increases to compress the two cellular structures in X direction to lead to the expansion of CS2 and contraction of CS1 in Y direction. The rear CS2 goes down to contact the ground with rear casing to produce a large friction f_2 to anchor to the ground. The front CS1 lifts up and only the front casing contacts the ground to produce a small friction f_1. If the three forces satisfy the relation of $f_1 < f_a < f_2$, the rear extreme will anchor to the ground, the central body will elongate and push the front extreme to move forward. When deflating the central actuator, the direction of the actuation force and the move direction of cellular structures will all change. The front CS1 will go down to contact the ground with front casing to produce a large friction f_3 to anchor to the ground. The rear CS2 will lift up and only the rear casing contacts the ground to produce a small friction f_4. If the three forces satisfy the relation of $f_4 < f_a < f_3$, the front extreme will anchor to the ground, the central body will contract and the rear extreme will move forward. Once deflation is done, the earthworm completes one cycle of peristaltic motion.

Based on the conceptual design, each part of the earthworm will be presented in details. As for central body, any linear actuator with sufficient force is able to drive the earthworm. A cylindrically symmetric bellow-like actuator is designed to simplify the case.

B. Extremes Design

Details about the structures of the extremes should be determined after conceptual design. Among the NPR cellular structures, re-entrant cellular structures stand out because the PR is tunable. The PR of a re-entrant cellular structure can be determined by the length of re-entrant strut, the length of side strut and the interior angle. For a unit cell in this study, the PR can only be determined by the interior angle. To find the relationship between unit cell interior angle and its Poisson's ratio, unit cell structure is analyzed. The unit cell structure shown in Fig. 2(a) with dimension of 20 mm × 20 mm is modeled in SOLIDWORKS, ABAQUS is used to simulate the behavior of the unit cell. Under the boundary conditions, the right edge is constrained in X direction and the top edge is constrained in Y direction. With a uniform input displacement applied on the left edge in X direction, an output displacement in the bottom direction could be found. The X direction displacement of the left edge and the Y direction displacement of the bottom edge are constrained to be uniform. The Poisson's ratio ν of the unit cell can be directly calculated by

$$\nu = -Dis\_out / Dis\_in. \tag{1}$$

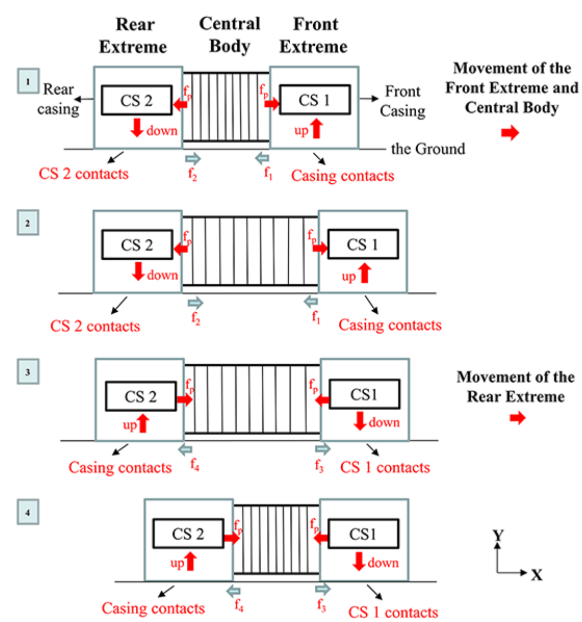

Fig. 1 Schematic diagram of the proposed earthworm with cellular structures.

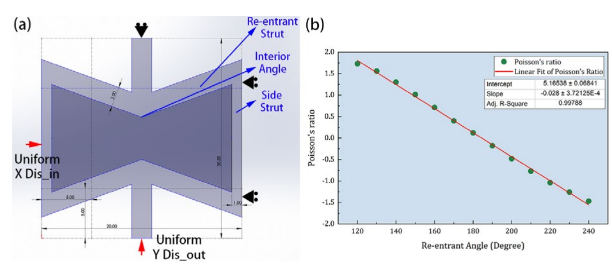

Fig. 2 (a) A re-entrant cellular structure unit cell with boundary conditions and (b) Linear fit of the Poisson's ratio with different angles.

Dis_out is the output displacement in the upward direction and *Dis_in* is the input-displacement in right edge direction.

To achieve a broader range of Poisson's ratio v, the interior angle θ is varied from 120° to 240°. Assumed as linear elastic deformation, 3D printable rubber-like material (TPU, Ninjaflex) with Young's modulus of 12 MPa and Poisson's ratio of 0.34 is chosen as the base material. As described in [21], there is a one-to-one corresponding relationship between v and θ if the applied strain lies in 0.15 and 0.3. Geometrically Nonlinear Finite Element Analysis of 13 unit cells with different angles is conducted to find the relationship between PR v and the interior angle θ under the nominal strain $\varepsilon = 0.15$. Once an interior angle is set, a corresponding output displacement can be achieved with the giving input displacement and its Poisson's ratio can be calculated. In this study, the Poisson's ratios are calculated with range from -1.47 to 1.73. By linear fitting of the Poisson's ratio as shown in Fig. 2(b), the relationship between the interior angle and Poisson's ratio can be described as

$$v = -0.028 \times \theta + 5.16538 \tag{2}$$

The deformation of cellular structures influences the anchoring movement of the earthworm. To make the cellular structures robust and ensure the friction produced by the cellular structures is large enough, 2 × 2 unit cells uniform normal and re-entrant cellular structures are selected. Normal cellular structures are lattice structures with positive PR. Each unit cell is assumed as isotropic and linear elastic. The final Poisson's ratio value is only related to interior angle and the applied strain as shown in Fig. 2(b).

To ensure symmetric force and deformation in front and rear extremes, the two cellular structures should have identical Young's moduli, and Poisson's ratios of equal magnitude but opposite phase. Poisson's ratios with value around ±1 are chosen for simplicity. Poisson's ratios with value around ±1 mean both extremes can produce the same output displacement as input displacement. By using (2) with Poisson's ratio equal to ±1, the interior angles of 149° and 220° are mapped for CS2 and CS1 respectively.

C. Gait Design

Fig. 3 shows the schematic diagram of a complete forward stride of peristaltic motion. It contains four phases. In Phase 1, the central actuator inflates to make the CS2 anchors to the ground, allowing the central body and front extreme move forward. In Phase 2, the central actuator achieves the largest elongation. Then it starts to deflate as shown in Phase 3. In this phase, the CS1 anchors to the ground to allow the rear extreme and central body to move forward. Finally, the central actuator finishes deflation to make the central body to recover to the original length to finish one cycle of gait as shown in Phase 4.

D. Materials and Fabrication

The assembly of the proposed earthworm at rest with all accurate components is shown in Fig. 4. The central body and cellular structures are printed by a commercial Fused deposition modeling (FDM) 3D printer (BCN3D Sigama, BCN3D Inc.). The materials used are both 3D printable flexible Thermoplastic Polyurethane (TPU) filaments. The casings are printed by a desktop 3D printer (Ultimaker 2+, Ultimaker Inc.). The materials used are Polylactic Acid (PLA) filaments.

The dimension of the whole earthworm is 160.14 mm × 41 mm × 46 mm. The central body consists of 12 unit of bellows. The middle eight normal-size bellows are designed for elongating movement, the two larger bellows with diameter of 35 mm are designed to connect with two casings by using epoxy resin AB glue. The remaining two normal bellows at two sides are designed to produce displacement to deform the cellular structures. The full length of central body is 72.32 mm. The diameter of the large hoops in normal bellows is 33 mm, the small hoops is 27 mm, and the wall thickness is 1 mm. The two casings have the dimension of 58.87 mm × 41 mm × 46 mm. One normal cellular structure and one re-entrant cellular structure are encapsulated into the two casings respectively. The normal cellular structure has 2 × 2 unit cells with a pad of 8 mm × 3 mm to contact the ground to produce friction, while the re-entrant cellular structure has 2 × 2 unit cells with a pad of 8 mm × 5 mm to contact the ground to produce friction. In order to enlarge the contacting area for more friction, the thickness of the two cellular structures is chosen as 12 mm. Two cellular structures are also inserted into guide grooves to simulate boundary conditions. The two casings and central body is glued as a whole, while two cellular structures can be assembled and disassembled.

The re-entrant cellular structure in the front extreme is designed to be in contact with the ground, while the normal cellular structure in the rear extreme has a distance of 2 mm above the ground at rest as shown in Fig. 4. It means the rear

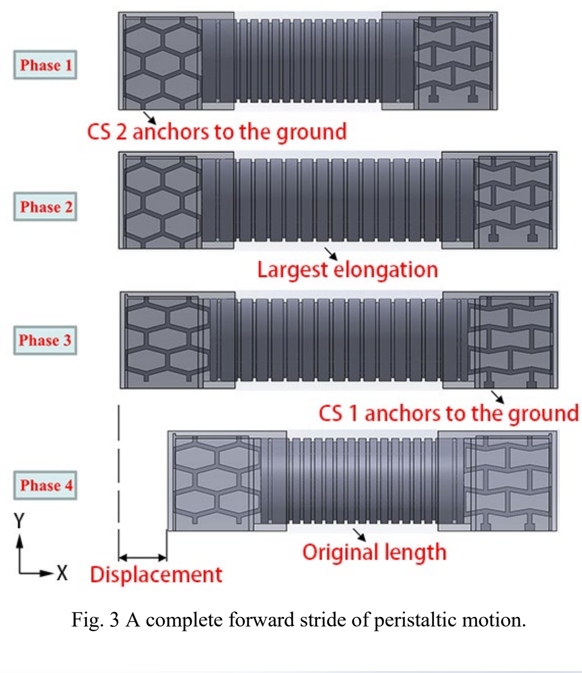

Fig. 3 A complete forward stride of peristaltic motion.

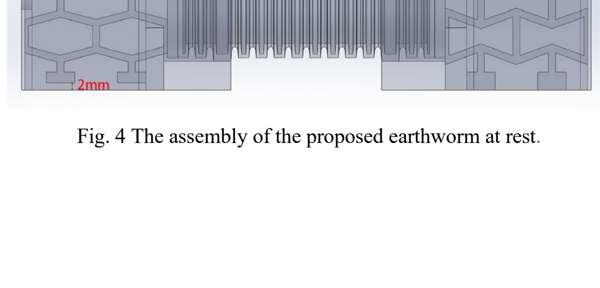

Fig. 4 The assembly of the proposed earthworm at rest.

extreme can only achieve anchoring movement when deformation of normal cellular structure is larger than 2 mm upon inflation.

III. Modeling of the Earthworm

Modeling of the earthworm is based on Finite Element Analysis (FEA). FEA is especially useful for analyzing the deformation of soft robot powered by pneumatic actuator and is used to predict the deformation of the earthworm.

A. *Modeling of the Pneumatic Actuator*

The model of central body pneumatic actuator is first established in SOLIDWORKS and then analyzed in ABAQUS.

Fig. 5 shows the model of the pneumatic actuator. Fig. 5(a) shows the main view of the actuator with eight normal bellows to produce elongating movement. One normal bellow is used to analyze the elongation of central body as shown in Fig. 5(b). When inflating the central body, the changes of their inner pressure result only in longitudinal displacements for axisymmetric bellows. The circumferential deformation is negligible. By summing up the total elongation of eight normal bellows, the simulated elongation for the pneumatic actuator can be found. To simplify the simulation, the normal bellow is divided into identical two halves. Fig. 5(c) shows one half of the unit bellow meshed into seeds.

The FEA is conducted to simulate the motion of pneumatic actuator under the assumption that the material is uncompressible and isotropic. Assumed as linear elastic, the TPU material (BCN3D) with Young's modulus of 40 MPa and Poisson's ratio of 0.34 is set as the base material in ABAQUS. The deformation of the half unit bellow is analyzed by giving constraint on circular plane. The influence of gravity is neglected, and uniform perpendicular pressure is given to the inner faces of the actuator to simulate the pressure provided by the pump. The influence of different input pressure on the elongation of the central body will be analyzed in the Simulation Results section.

B. *Modeling of Anchoring Movement*

Anchoring movement is achieved by switching the contacting surface of two extremes with the ground. The TPU soft cellular structure has a high coefficient of friction with the ground, while the PLA hard casing has a low coefficient of friction with the ground. To achieve anchoring movement, the displacement of CS2 in rear extreme should be larger than 2 mm. The input displacements for cellular structures in X direction are set to 3 mm to satisfy the requirement of applied strain of 0.15. The design of the inner structure of casings constrains the input displacement to 3 mm. The output displacement should be calculated as 3 mm for the two cellular structures, which provides enough distance for CS2 to contact the ground.

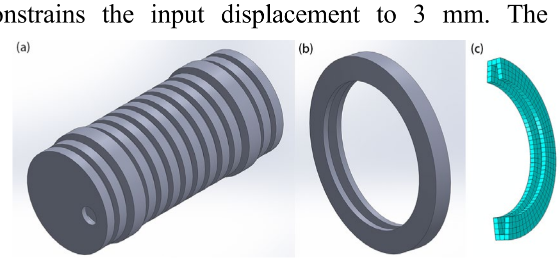

Fig. 5 The model of the pneumatic actuator. (a) the main view, (b) a normal-size bellow in the middle part and (c) half of the meshed normal bellow.

In this part, the FEA model of the CS1 and CS2 are established to predict the output displacement in Y direction to see whether CS1 and CS2 satisfy the requirement of 2 mm displacement in anchoring movement.

Fig. 6 shows the model of 2 × 2 normal and re-entrant cellular structures with interior angle of 149° and 220°. The normal cellular structure CS2 expands in Y direction under compression in X direction, while the re-entrant CS1 clearly contracts in Y direction when compressing in X direction. Fig. 6(a) and Fig. 6(c) show the boundary conditions of each cellular structure. Both right edges are constrained in X direction, and both top edges are constrained in Y direction. Input displacements are given to the left edges in X directions. The output displacements of bottom edges are the required deformation. After given boundary conditions, the two structures are meshed into seeds as shown in Fig. 6(b) and Fig. 6(d).

IV. Simulation Results

A. *Deformation of the Pneumatic Actuator*

To research the relationship between pressure and elongation, the deformation of half unit bellow under different pressures is used as shown in Fig. 7. Through FEA, one unit bellow is found to be deformed in longitudinal direction at 1.19 mm under the pressure of 3 kPa. When increasing the

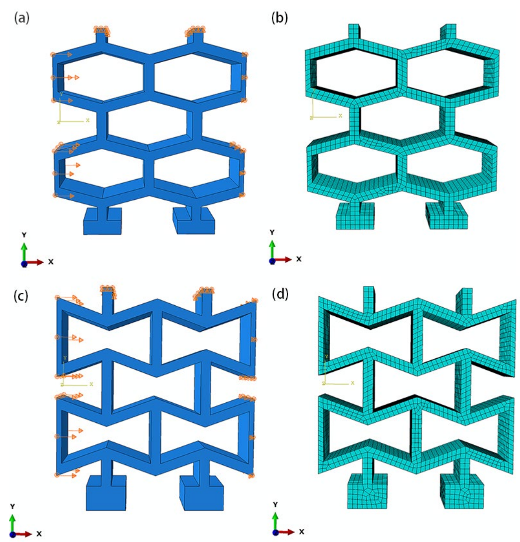

Fig. 6 The model of normal cellular structure (a) with boundary conditions (b) meshed into seeds and re-entrant cellular structure (c) with boundary conditions (d) meshed into seeds.

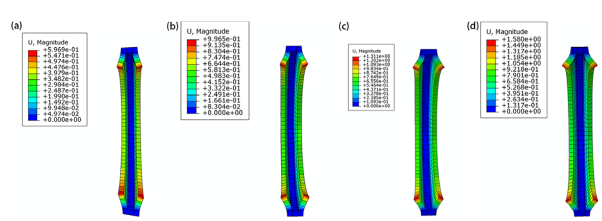

Fig. 7 The deformation images of half unit bellow under the pressure of (a) 3 kPa, (b) 6 kPa, (c) 9 kPa and (d) 12 kPa.

pressure from 3 kPa to 12 kPa, the longitudinal displacement increases accordingly as shown from Fig. 7(a) to Fig. 7(d).

After getting the elongation of one bellow, the whole elongation of the pneumatic actuator can be found by summing up the displacements of eight middle bellows under the assumption of linear pneumatic actuator. The relationship between the pressure and elongation for central body is established and plotted in Fig. 8. Almost linear relationship between pressure and elongation can be seen from the figure. It indicates that it is reasonable to assume the linear actuator design in Section 2 and to sum up eight bellows for total elongation. For the input pressure of 3 kPa, the whole elongation for the pneumatic actuator reaches 9.5504 mm. The prototype test will be conducted under this pressure to validate the model.

B. *Deformation of the Cellular Structures in Anchoring Movement*

As shown in Fig. 9(a), the normal cellular structure moves down 5.236 mm in Y direction under the input displacement of 3 mm in X direction. It's larger than the distance of 2 mm for normal cellular structure to touch the ground mentioned in Section 2. The output displacement of the re-entrant cellular structure is nonuniform in the simulation as shown in Fig. 9(b). One pad lifts up 3.498 mm, while the other lifts up 6.05 mm in Y direction. There is a possibility that the interactive forces of each unit cell in the 2 × 2 cellular structures contribute to the discrepancy. From the simulation results of CS1 and CS2, the two extremes can both achieve anchoring movement and moving forward.

V. TESTING

In order to validate the proposed design and modeling of single pneumatic actuator and cellular structures, an earthworm capable of peristaltic motion is fabricated and tested. Fig. 10 shows the prototype of the earthworm after assembly. The total length of the earthworm in longitudinal direction is 160.14 mm as illustrated in fabrication section. A silicone tube with diameter of 6 mm is used to connect the actuator to a pump which supplies pressure to inflate and deflate the earthworm as seen at the rear extreme.

In this system, air pump (370-B, DC 6.0 V, 150 kPa) works as air source to inflate the central actuator. A valve is used to control the air input and output. Manual control is used to adjust the state of inflation and deflation. The earthworm is put on a board with grids and scales as shown in Fig. 11. The displacements for one cycle can be calculated by measuring the coordinates from the start to the end in one direction.

Under actuation, the fabricated earthworm is able to move with peristaltic motion. Supplementary Movie S1 shows one cycle of the earthworm achieving peristaltic motion from the front and top views when the air pressure is 3 kPa. In order to satisfy the friction relations in Section 2 for anchoring and movement of the earthworm, weights are added on two extremes. In one cycle, Fig. 11(a) shows the original state of the earthworm. Fig. 11(b) shows the rear extreme anchors to the ground, the central body achieves its largest elongation and the front extreme moves forward after inflation. It starts to deflate to switch the anchor surface. As the actuator is fully deflated as shown in Fig. 11(c), the front extreme anchors to the ground, the central body contracts to the original length, and the rear extreme moves forward. The earthworm achieves continuous peristaltic motion by repeating cycles of inflation and deflation.

The displacement of a complete peristaltic motion cycle can also be measured as seen in the figures. With the position

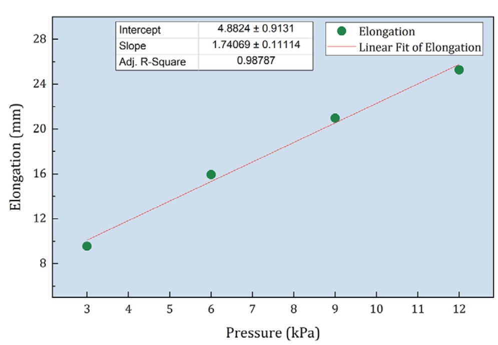

Fig. 8 The relationship between actuation pressure and elongation.

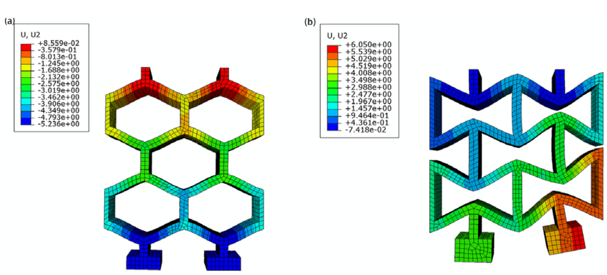

Fig. 9 The deformation images of (a) normal and (b) re-entrant cellular.

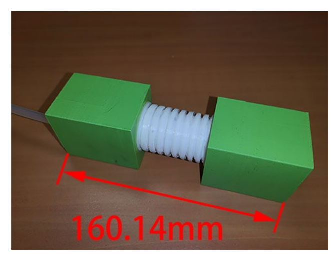

Fig. 10 The prototype of the earthworm.

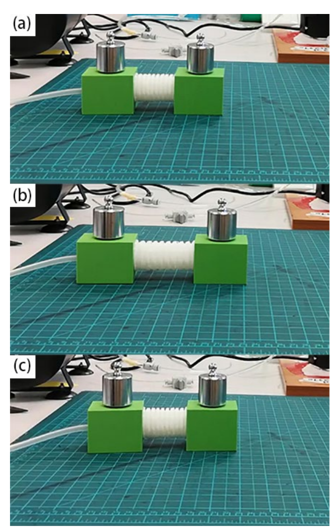

Fig. 11 One cycle of movement for the earthworm prototype under the pressure of 3 kPa.

of the front edge of the front extreme from Fig. 11(a) at the coordinate of 217 mm to Fig. 11 (c) at the coordinate of 226 mm in longitudinal direction on the grid board, the displacement of 9 mm is achieved in one cycle.

The simulation model predicts the elongation of the earthworm for one cycle as 9.5504 mm. Comparing with the experimental results, the difference in elongation with the simulated ones is calculated as 5.8 %. The discrepancy could be due to the fabrication quality of the central body that affects the elongation result. The imperfect in gluing each part may also cause the discrepancy. The anchoring parts with CSs and hard casings may also contribute to the discrepancy. The sliding effect of two contacting surfaces are not considered in the analysis of peristaltic motion.

Compared to similar type of earthworms with more pumps and chambers, the proposed earthworm may have reduced flexibility in movement as there is only one pump and valve to control both elongating and anchoring movement. However, it is easier to control the motion of earthworms with single pneumatic actuator and cellular structures. The movement speed could also be improved as the time for the control of anchoring motion is reduced. Detailed experiments to compare speed differences will be conducted in the future to validate the analysis. Overall, the earthworm with proposed design of single pneumatic actuator and cellular structures proves to be feasible to achieve the peristaltic motion.

VI. Conclusion

In this work, we propose a novel design of integrating single pneumatic actuator and cellular structures to achieve peristaltic motion in earthworm-like soft robot. The earthworm consists of three sections, the front extreme, central body and the rear extreme. Cellular structures with different Poisson’s ratio are integrated with the single actuator to achieve anchoring movement. Simulation models are established to predict the elongation of the pneumatic actuator and the deformation of cellular structures. Almost linear relationship between the input pressure and elongation of the central body is established and anchoring movement is successfully predicted by simulation model. To validate the proposed design and modeling, an earthworm prototype is fabricated. Experimental results show that the earthworm can achieve both anchoring and elongation movements to moving forward. Further, the experimental displacement of one cycle movement is agreeable with the predicted displacement from the simulated model.

In the future, the relationship between the actuation pressure and moving velocity of the earthworm will be studied. More comparable experiments will be conducted to validate the new design and simulations.

Acknowledgment

M. Liu would like to thank you for the financial support from China Scholarship Council (CSC) under the grant No. 201706050146.

References

[1] Yousef, H., Boukallel, M., & Althoefer, K. (2011). Tactile sensing for dexterous in-hand manipulation in robotics—A review. *Sensors and Actuators A: physical, 167*(2), 171-187.

[2] Ren, Z., Hu, W., Dong, X., & Sitti, M. (2019). Multi-functional soft-bodied jellyfish-like swimming. *Nature communications*, 10(1), 1-12.

[3] Zheng, T., Branson, D. T., Guglielmino, E., Kang, R., Medrano Cerda, G. A., Cianchetti, M., ... & Caldwell, D. G. (2013). Model validation of an octopus inspired continuum robotic arm for use in underwater environments. *Journal of Mechanisms and Robotics*, 5(2).

[4] Zou, J., Lin, Y., Ji, C., & Yang, H. (2018). A reconfigurable omnidirectional soft robot based on caterpillar locomotion. *Soft robotics*, 5(2), 164-174.

[5] Donatelli, C. M., Serlin, Z. T., Echols-Jones, P., Scibelli, A. E., Cohen, A., Musca, J. M., ... & Trimmer, B. A. (2017, September). Soft foam robot with caterpillar-inspired gait regimes for terrestrial locomotion. In *2017 IEEE/RSJ International Conference on Intelligent Robots and Systems (IROS)* (pp. 476-481). IEEE.

[6] Sun, Z., Yamauchi, Y., Araoka, F., Kim, Y. S., Bergueiro, J., Ishida, Y., ... & Aida, T. (2018). An Anisotropic Hydrogel Actuator Enabling Earthworm‐Like Directed Peristaltic Crawling. *Angewandte Chemie*, 130(48), 15998-16002.

[7] Yim, S., & Sitti, M. (2011). Design and rolling locomotion of a magnetically actuated soft capsule endoscope. *IEEE Transactions on Robotics, 28*(1), 183-194.

[8] Zhang, Z., Wang, X., Wang, S., Meng, D., & Liang, B. (2019). Design and Modeling of a Parallel-Pipe-Crawling Pneumatic Soft Robot. *IEEE Access, 7*, 134301-134317.

[9] Seok, S., Onal, C. D., Wood, R., Rus, D., & Kim, S. (2010, May). Peristaltic locomotion with antagonistic actuators in soft robotics. In *2010 IEEE International Conference on Robotics and Automation* (pp. 1228-1233). IEEE.

[10] Huang, W. (2002). On the selection of shape memory alloys for actuators. *Materials & design*, 23(1), 11-19.

[11] Pelrine, R., Kornbluh, R., Joseph, J., Heydt, R., Pei, Q., & Chiba, S. (2000). High-field deformation of elastomeric dielectrics for actuators. *Materials Science and Engineering: C, 11*(2), 89-100.

[12] Qi, Q., Teng, Y., & Li, X. (2015, August). Design and characteristic study of a pneumatically actuated earthworm-like soft robot. In *2015 International Conference on Fluid Power and Mechatronics (FPM)* (pp. 435-439). IEEE.

[13] Calderón, A. A., Ugalde, J. C., Zagal, J. C., & Pérez-Arancibia, N. O. (2016, December). Design, fabrication and control of a multi-material-multi-actuator soft robot inspired by burrowing worms. In *2016 IEEE international conference on robotics and biomimetics (ROBIO)* (pp. 31-38). IEEE.

[14] Banhart, J. (2001). Manufacture, characterisation and application of cellular metals and metal foams. *Progress in materials science*, 46(6), 559-632.

[15] Abate, K. M., Nazir, A., Yeh, Y. P., Chen, J. E., & Jeng, J. Y. (2020). Design, optimization, and validation of mechanical properties of different cellular structures for biomedical application. *The International Journal of Advanced Manufacturing Technology*, 106(3-4), 1253-1265.

[16] Lim, T. C. (2015). *Auxetic materials and structures*. Singapore: Springer.

[17] Mark, A. G., Palagi, S., Qiu, T., & Fischer, P. (2016, May). Auxetic metamaterial simplifies soft robot design. In *2016 IEEE International Conference on Robotics and Automation (ICRA)* (pp. 4951-4956). Ieee.

[18] Hasse, A., & Mauser, K. (2019). Poisson Induced Bending Actuator for Soft Robotic Systems. *Soft robotics*.

[19] Lazarus, A., & Reis, P. M. (2015). Soft actuation of structured cylinders through auxetic behavior. *Advanced Engineering Materials*, 17(6), 815-820.

[20] Joey, Z. G., Calderón, A. A., Chang, L., & Pérez-Arancibia, N. O. (2019). An earthworm-inspired friction-controlled soft robot capable of bidirectional locomotion. *Bioinspiration & biomimetics*, 14(3), 036004.

[21] Han, Y., & Lu, W. (2018). Evolutionary design of nonuniform cellular structures with optimized Poisson's ratio distribution. *Materials & Design*, 141, 384-394.